3-D Flow Effects on Residence Time Distribution in Screw Extruders

L. Chen and J. T. Lindt
Dept. of Materials Science and Engineering, University of Pittsburgh, Pittsburgh, PA 15261

This work concerns some selected 3-D flow effects on residence time distribution (RTD) in a screw extruder. The Newtonian problem is emphasized in which the cross- and down-channel flow components can be formally discoupled and treated as two parallel 2-D problems: our stream-function-based analysis of the Newtonian cross-channel flow was combined with the existing 2-D solution for the down-channel flow. The RTD was determined by tracing the streamlines generated from both velocity components for the industrially important cases of fully- and partially-filled channels. The effect of the cross-channel flow on the RTD is discussed in connection with the stagnation flows, the down-channel pressure gradient, and the presence of a free surface in a partially-filled channel. The cross-channel pressure distribution is compared to the conventional 1-D theory. The non-Newtonian effects were assessed using the commercial software POLYCAD.

Introduction

Hydrodynamic analysis of flows in a screw pump has been studied in the context of polymer extrusion since the early 1950s. For a Newtonian flow in a straight rectangular channel, the equation of motion was solved early for the unidirectional down-channel flow by the separation of variables method (McKelvey, 1962). The average down-channel velocity and the volumetric pumping rate were obtained by integrating the velocity field over the channel cross section.

Analysis of the flow across the channel was usually simplified by assuming that the channel aspect ratio (width/depth ratio) is so large that the cross-channel flow is unaffected by the side walls and the flow description in one dimension is adequate (McKelvey, 1962; Tadmor and Klein, 1970). More accurate solutions, involving the circulatory motions in the vicinity of the side walls, were largely overlooked due to the mathematical complications involved.

An understanding of the cross-channel flow is important for a multitude of extrusion processes where the aspect ratio of the channel (W/H) and/or the melt pool (W_s/H) may not or cannot be large enough for the cross-channel flow to be considered to be one-dimensional. The aspect ratio of the channel cross section filled with melt tends to be small for a melt pool in the melting zone of a screw extruder, and for partially-filled channels in any extrusion process that includes devolatilization. Accurate cross-channel flow analysis becomes a prerequisite for simulations of RTD functions in such cases.

In the conventional analysis of the RTD, the effect of the screw flights was neglected, regardless of the significant errors introduced into the analysis. For example, 1-D flow was assumed in a channel of an intermeshing counterrotating twin screw extruder where the aspect ratio can be as small as 1.6 (Chen and Pan, 1993). An average down-channel velocity was used to evaluate the RTD in a partially-filled channel in a corotating twin screw extruder (Kao and Allison, 1984).

An accurate analysis of the cross-channel flow remains a problem. Burggarf (1966) introduced the stream and vorticity functions into the 2-D equation of motion to study the flow of low viscosity fluids in a rectangular channel similar to the channels in screw extruders. A somewhat similar analysis also appeared two decades later (Leong and Ottino, 1989) with no specific reference to the free surface present in the partially-filled channel. These methods have not been introduced into the conventional polymer processing analysis due to the mathematical complexities involved.

The objective of this work is to analyze the cross-channel flow and develop a model for the RTD in channels with moderate and small aspect ratios. The 2-D equation of motion for the cross-channel flow, together with the boundary condi-

Correspondence concerning this article should be addressed to J. T. Lindt.
Current address of L. Chen: BICC Cables Corp., Indianapolis Technology Center, Indianapolis, IN 46214.

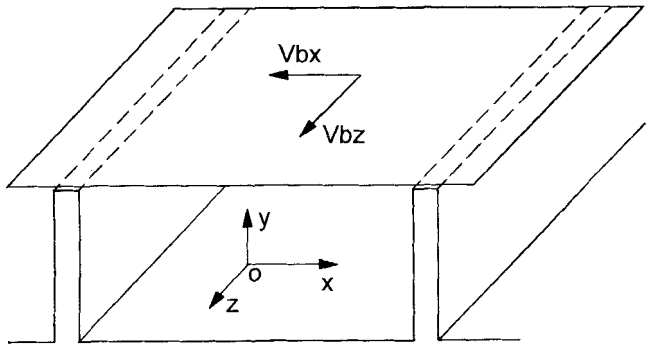

Figure 1. Flow in single screw extruder.

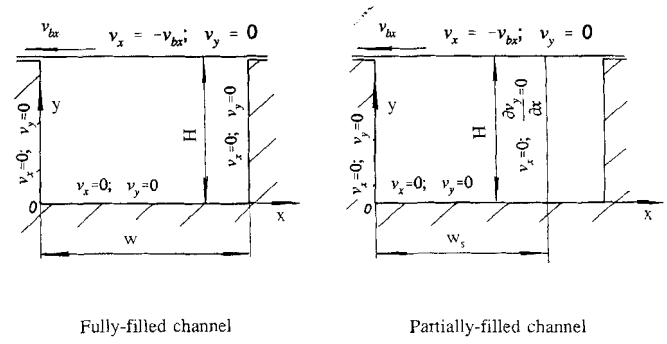

Figure 2. Cross-channel flow and boundary conditions.
(a) Fully-filled channel; (b) partially-filled channel.

tions for both a fully-filled channel (without free surface) and a partially-filled channel (with free surface), was solved by introducing the stream function and applying a finite difference method, allowing the effect of cross-channel flow on the RTD to be further discussed.

Analysis

Hydrodynamics of the cross-channel flow

For highly viscous Newtonian fluids, the flow in a single screw extruder may be treated in terms of the down-channel v_z and cross-channel v_x and v_y velocity components, as suggested in Figure 1. The down-channel flow has been well studied (McKelvey, 1962). The cross-channel flow can be described by the 2-D form of the equation of motion (Figure 2)

$$\mu\left(\frac{\partial^2 v_x}{\partial x^2}+\frac{\partial^2 v_x}{\partial y^2}\right)=\frac{\partial p}{\partial x}$$
$$\mu\left(\frac{\partial^2 v_y}{\partial x^2}+\frac{\partial^2 v_y}{\partial y^2}\right)=\frac{\partial p}{\partial y} \qquad (1)$$

along with the equation of continuity

$$\frac{\partial v_x}{\partial x}+\frac{\partial v_y}{\partial y}=0 \qquad (2)$$

Assuming a rectangular channel these equations are subject to the following boundary conditions for a fully-filled channel (Figure 2a)

$$\begin{aligned}
&@\ x=0: && v_x=0, && v_y=0;\\
&@\ y=0: && v_x=0, && v_y=0;\\
&@\ x=W: && v_x=0, && v_y=0\\
&@\ y=H: && v_x=-v_{bx}, && v_y=0
\end{aligned} \qquad (3)$$

or alternatively for a partially-filled channel (Figure 2b) to

$$\begin{aligned}
&@\ x=0: && v_x=0, && v_y=0;\\
&@\ y=0: && v_x=0, && v_y=0;\\
&@\ x=W_s: && v_x=0, && \left(\frac{\partial v_y}{\partial x}\right)=0\\
&@\ y=H: && v_x=-v_{bx}, && v_y=0
\end{aligned} \qquad (4)$$

In Eqs. 3 and 4, W is the screw channel width, W_s is the filled width in the partially-filled channel, H is the channel depth, and v_{bx} is barrel velocity in x direction. The rectangular channel assumption may introduce some error for the partially-filled channel, because the free surface is not straight. This error may become significant if the width/depth ratio of the polymer ribbon becomes too small.

Equations 1 and 2 are coupled partial differential equations in three unknowns: the velocity components $v_x(x,y)$ and $v_y(x,y)$, and pressure $p(x,y)$. These equations are difficult to separate and have to be solved simultaneously. In this work, they were solved by introducing the stream function ψ defined as follows

$$v_x=-\frac{\partial \psi}{\partial y}$$
$$v_y=\frac{\partial \psi}{\partial x} \qquad (5)$$

Introducing Eq. 5 into Eq. 1 yields

$$v\left(\frac{\partial^4 \psi}{\partial x^4}+2\frac{\partial^4 \psi}{\partial x^2 \partial y^2}+\frac{\partial^4 \psi}{\partial y^4}\right)=0 \qquad (6)$$

to be treated with the following boundary conditions (c.f. Eq. 3) for a fully-filled channel

$$\begin{aligned}
&@\ =o: && v_x=-\frac{\partial \psi}{\partial y}=0; && v_y=\frac{\partial \psi}{\partial x}=0\\
&@\ y=0: && v_x=-\frac{\partial \psi}{\partial y}=0; && v_y=\frac{\partial \psi}{\partial x}=0\\
&@\ x=w_s: && v_x=-\frac{\partial \psi}{\partial y}=0; && v_y=\frac{\partial \psi}{\partial x}=0\\
&@\ y=H: && v_x=-\frac{\partial \psi}{\partial y}=-v_{bx}; && v_y=\frac{\partial \psi}{\partial x}=0
\end{aligned} \qquad (7)$$

or with the following (c.f. Eq. 4) for a partially-filled channel

$$
\begin{aligned}
&@\ x=o: \quad v_x=-\frac{\partial\psi}{\partial y}=0; && v_y=\frac{\partial\psi}{\partial x}=0\\
&@\ y=0: \quad v_x=-\frac{\partial\psi}{\partial y}=0; && v_y=\frac{\partial\psi}{\partial x}=0\\
&@\ x=w_s: \quad v_x=-\frac{\partial\psi}{\partial y}=0; && \frac{\partial v_y}{\partial x}=\frac{\partial^2\psi}{\partial x^2}=0\\
&@\ y=H: \quad v_x=-\frac{\partial\psi}{\partial y}=-v_{bx}; && v_y=\frac{\partial\psi}{\partial x}=0
\end{aligned} \tag{8}
$$

Equations 6–8 have been solved using the finite differences

$$
\frac{\partial^4\psi}{\partial y^4}=\frac{\psi_{j+2}-4\psi_{j+1}+6\psi_j-4\psi_{j-1}+\psi_{j-2}}{\Delta x^4}
$$

$$
\frac{\partial^4\psi}{\partial x^4}=\frac{\psi_{i+2}-4\psi_{i+1}+6\psi_i-4\psi_{i-1}+4\psi_{i-2}}{\Delta x^4}
$$

$$
\frac{\partial^4\psi}{\partial x^2\partial y^2}=\frac{\psi_{i+1,j+1}-2\psi_{i,j+1}+\psi_{i-1,j+1}-2(\psi_{i+1,j}-2\psi_{i,j}+\psi_{i-1,j})+\psi_{i+1,j-1}-2\psi_{i,j-1}+\psi_{i-1,j-1}}{\Delta x^2\Delta y_2} \tag{9}
$$

allowing Eq. 6 to be replaced by

$$
\frac{\psi_{i+2,j}-4\psi_{i+1,j}+6\psi_{i,j}-4\psi_{i-1,j}+\psi_{i-2,j}}{\Delta x^4}+\frac{\psi_{i,j+2}-4\psi_{i,j+1}+6\psi_{i,j}-4\psi_{i,j-1}+\psi_{i,j-2}}{\Delta y^4}
$$

$$
+2\,\frac{\psi_{i+1,j+1}-2\psi_{i,j+1}+\psi_{i-1,j+1}-2(\psi_{i+1,j}-2\psi_{i,j}+\psi_{i-1,j})+\psi_{i+1,j-1}-2\psi_{i,j-1}+\psi_{i-1,j-1}}{\Delta x^2\Delta y^2}=0 \tag{10}
$$

to be finally solved by Gauss-Seidel iteration with relaxation, based on the following explicit formula

$$
\begin{aligned}
\psi_{i,j}=\frac{1}{20}\,[&8(\psi_{i+1,j}+\psi_{i-1,j}+\psi_{i,j+1}+\psi_{i,j-1})\\
&-2(\psi_{i+1,j+1}+\psi_{i+1,j-1}+\psi_{i-1,j+1}+\psi_{i-1,j-1})\\
&-(\psi_{i+2,j}+\psi_{i-2,j}+\psi_{i,j+2}+\psi_{i,j-2})]
\end{aligned} \tag{11}
$$

Velocity profiles $v_x(x,y)$ and $v_y(x,y)$, pressure $p(x,y)$ and stresses can be recovered from the discrete values of the stream function using numerical approximations of the definitions given by Eqs. 1 and 5.

RTD in shallow channels

The RTD can be determined by tracking the streamlines whereby the trajectory is determined from the known velocity distribution in the x-y plane: $x=x(v_x,v_y,t)$ and $y=y(v_x,v_y,t)$, as described in the preceding section, and the traditional solution for the down-channel velocity profile $v_z(x,y)$ (Bernhardt, 1959). In other words, the time t spent by a given fluid particle in a channel of length L is determined by converting the velocity components v_x,v_y,v_z into the residence time spectrum through

$$
t=\int_0^L \frac{dz}{v_z(x,y)} \tag{12}
$$

making use of the conventional analytical solution for the down-channel velocity distribution

$$
\begin{aligned}
v_z=\frac{4v_{bz}}{\pi}\sum_{i=1,3,\ldots}^{\infty}\frac{\sinh(i\pi y/W)}{i\sinh(i\pi H/W)}\sin\left(\frac{i\pi x}{W}\right)-\frac{1}{\mu}\left(\frac{\partial p}{\partial z}\right)\\
\times\left[\frac{y^2}{2}-\frac{yH}{2}+\frac{4H^2}{\pi^3}\sum_{i=1,3,\ldots}^{\infty}\frac{\cosh\left[\left(\frac{i\pi}{2H}\right)(2x-w)\right]}{i^3\cosh\left(\frac{i\pi W}{H}\right)}\sin\left(\frac{i\pi y}{H}\right)\right]
\end{aligned} \tag{13}
$$

remembering that for a given fluid particle $v_z(x,y)$ varies with z as its location in the x-y plane change with z.

The volume fraction of fluid particles residing in the channel between time t and $t+dt$ is related to the down-channel velocity at the inlet through Eq. 14:

$$
f(t)dt=\frac{v_z(x,y)dA}{Q} \tag{14}
$$

where dA is the area at inlet within which the fluid particle resides between time t and $t+dt$, and $v_z(x,y)$ is the average velocity in dA.

Results and Discussion

Stream function, streamlines and stagnating flow

An example of the stream function obtained from Eq. 10 is shown in Figure 3. The streamlines, defined as the lines within the x-y plane along which the stream function has discrete constant values, are shown in Figure 4a for a fully filled channel and in Figure 4b for a partially-filled channel. Note that in the fully filled channel the streamline pattern is symmetrical, in contrast to the partially-filled channel where free surface exists.

Of interest is the sparsity of streamlines in both corners at the bottom of the channel. They indicate insignificant changes in the stream function and, therefore, relatively small cross-channel velocities. Moreover, Eq. 13 suggests that at these two locations the down-channel velocity is also small (Figure 5). Thus, a fluid particle will travel in the corners at the channel floor for a long time due to the small velocity in all three directions. The screw channels are usually rounded to prevent this type of stagnation. The radius of curvature R necessary to prevent stagnation can be estimated crudely from the

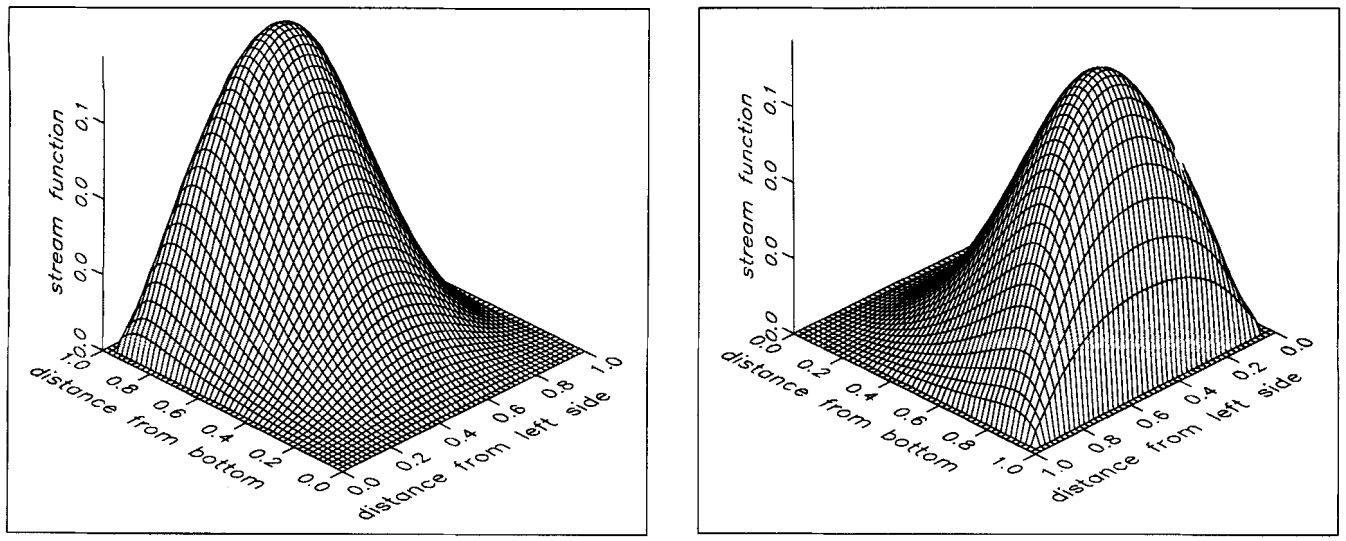

Figure 3. Stream function obtained from Eq. 10.

(a) Front view; (b) rear view.

streamline shape and density, leading to a value of about 1/4 of the channel depth H.

Figure 6 shows the streamlines for channels of different aspect ratios. It is interesting to note that the ratio of the radius of the stagnation area to the channel depth is almost constant for channels of aspect ratios between 1 and 10; for reference refer to Figure 4a showing a full set of streamlines for $W/H = 1$. Thus, the R/H ratio estimated as 1/4 appears to possess some generality. This ratio is affected however by non-Newtonian flow behavior, as shown in the Appendix.

If the screw channel is very narrow, the corner areas of stagnating flow become large. The segregated flows in the corners tend to come together and form a single vortex, as shown in Figure 7a. This further illustrates the fact that the stationary side wall can provide a significant flow resistance and effectively restrict the cross-channel circulation. With increasing flow stagnation, the fraction of the fluid trapped in the "dead" corners increases accordingly, with all due consequences for the RTD. Such narrow screw channels are not acceptable and as a rule are avoided in practice, needless to mention their inability to sufficiently pump and develop pressure.

In a partially-filled channel, however, the stagnation does not necessarily increase significantly even when the fillage

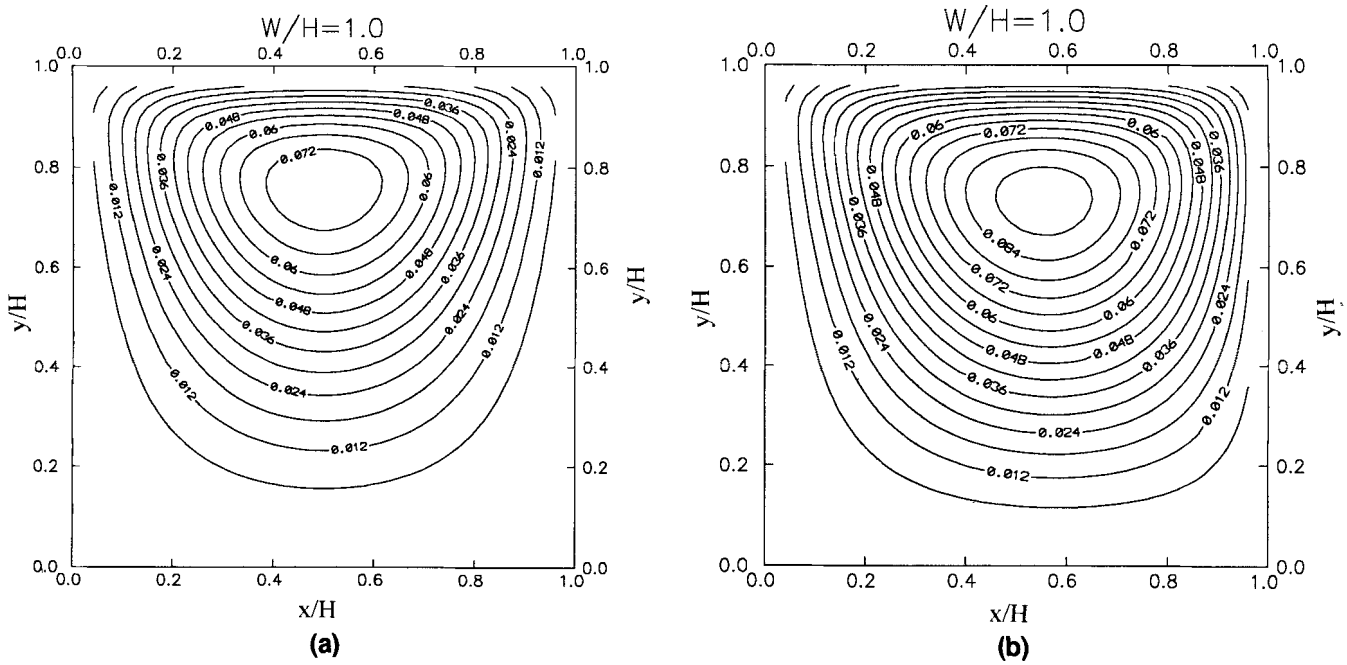

Figure 4. Streamlines from Eq. 10.

(a) Fully-filled channel; (b) partially-filled channel.

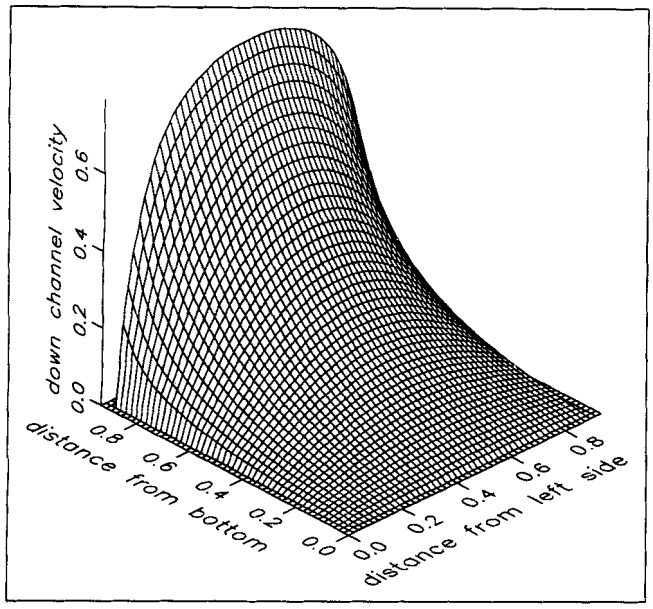

Figure 5. Down-channel velocity distribution in a fully-filled channel.

becomes small. Figure 7b supports the suggestion that the free surface does not pose an appreciable restriction to the circulation of the fluid. The streamlines remain virtually the same shape for the channel with $W/H < 1$. The radius of the rounded corner at the pushing flight, as estimated for flow in the fully filled channel, is also suitable for partially filled channels. This conclusion is important because the effective aspect ratio W_s/H can vary along the length of the channel and eventually become quite small. In particular, during devolatilization the liquid flow rate can drop precipitously with distance as large amounts of mass are removed through the vents. It should be borne in mind that the free surface is not perfectly flat as assumed here. The fact that the streamlines remain virtually unchanged by the introduction of the free surface in principle suggests, however, that minor variations in the shape of the free surface are not going to appreciably affect the flow at the pushing flight nor the RTD.

Pressure distribution

The conventional analysis of unidirectional, fully-developed Newtonian cross-channel flow (Eq. 6) gives that

$$\frac{\partial p}{\partial x} = 6\mu \frac{v_{bx}}{H^2}; \qquad \frac{\partial p}{\partial y} = 0 \tag{15}$$

thus a linear pressure profile across the channel width (x-direction), and constant pressure along the channel depth (y-direction).

Presently, the pressure distribution in the x-y plane has been obtained from the known stream function and Eqs. 1 and 5. Examples of the cross-channel pressure distributions are shown in Figures 8a and 8b for the aspect ratio equal to one. As expected, the constant pressure along the channel depth may only be observed locally, say, in the middle of the channel, and the linear pressure profile across the channel width may perhaps prevail over a relatively small area. Note that there is a sharp pressure change at the upper corners, brought about by the 2-D nature of the cross-channel flow.

The pressure difference at the channel top between the pushing and trailing flights in a fully-filled channel, or be-

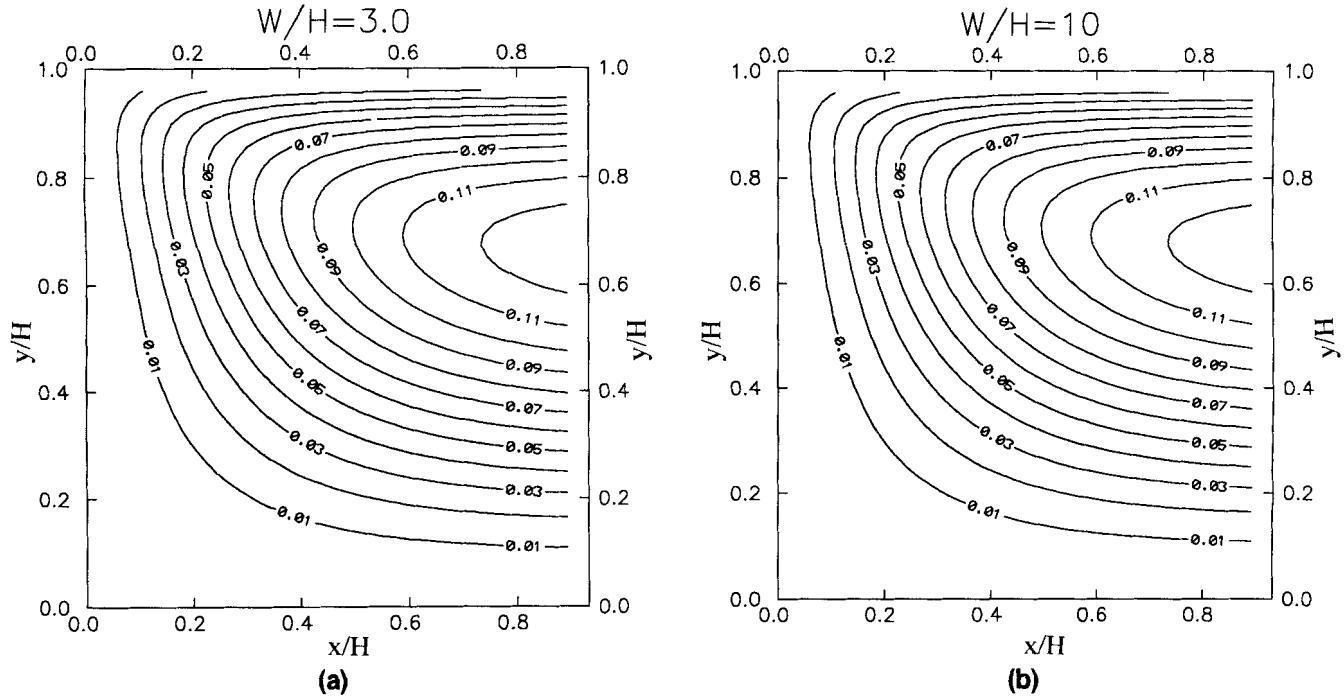

Figure 6. Streamlines in channels of different aspect ratios.

(a) $W/H = 3.0$; (b) $W/H = 10.0$.

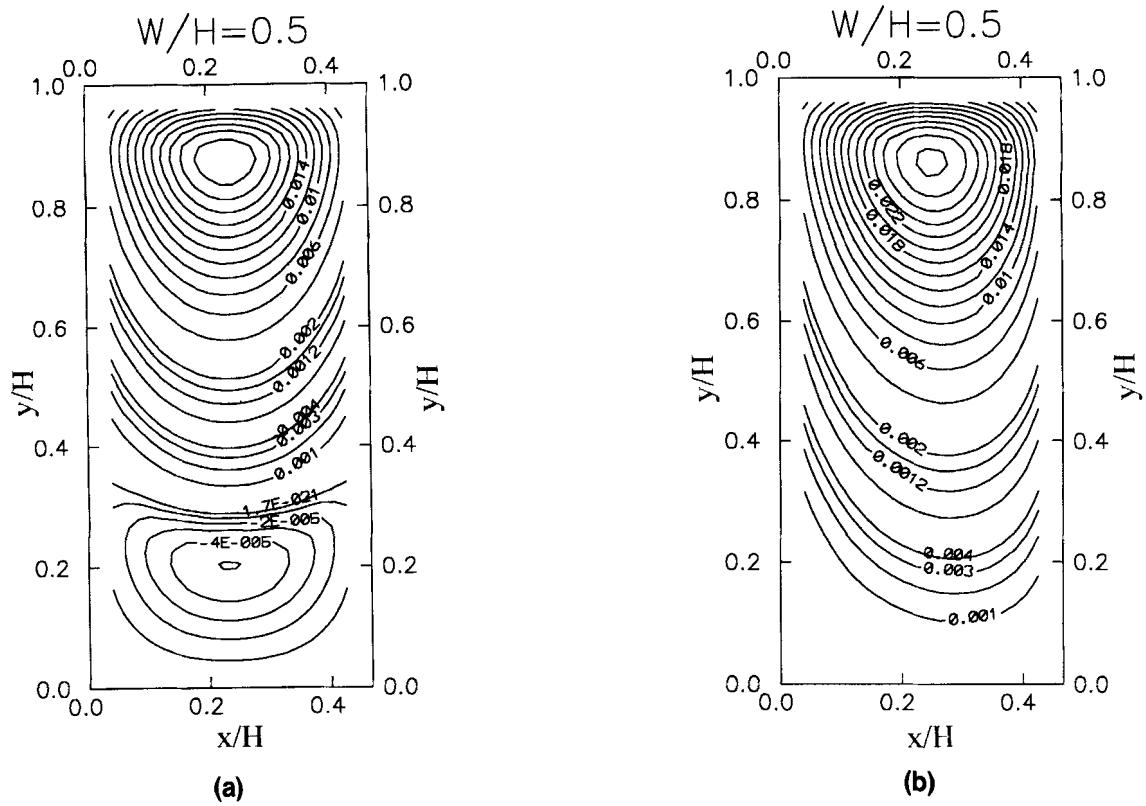

Figure 7. Streamlines in liquid domains with a small aspect ratio.

(a) Fully-filled channel; (b) partially-filled channel.

tween the pushing flight and local gas/vapor pressure in a partially-filled channel, contributes to the leakage flow over the screw flights. Table 1 shows the pressure differences in a fully-filled channel predicted by both this model and Eq. 15 in terms of the normalized pressure difference defined as

$$\frac{\Delta p H^2}{6\mu W v_{bx}} \tag{16}$$

The difference between the two models becomes significant with decreasing aspect ratio. This contribution plays a major role of the overall pressure development when W/H is small. Under such conditions, Eq. 15 becomes inaccurate and loses its utility.

Our results are relevant to analysis of leakage flow in narrow channels. Conceptually, this effect is clear but its inclusion in the overall extrusion analysis may be laborious.

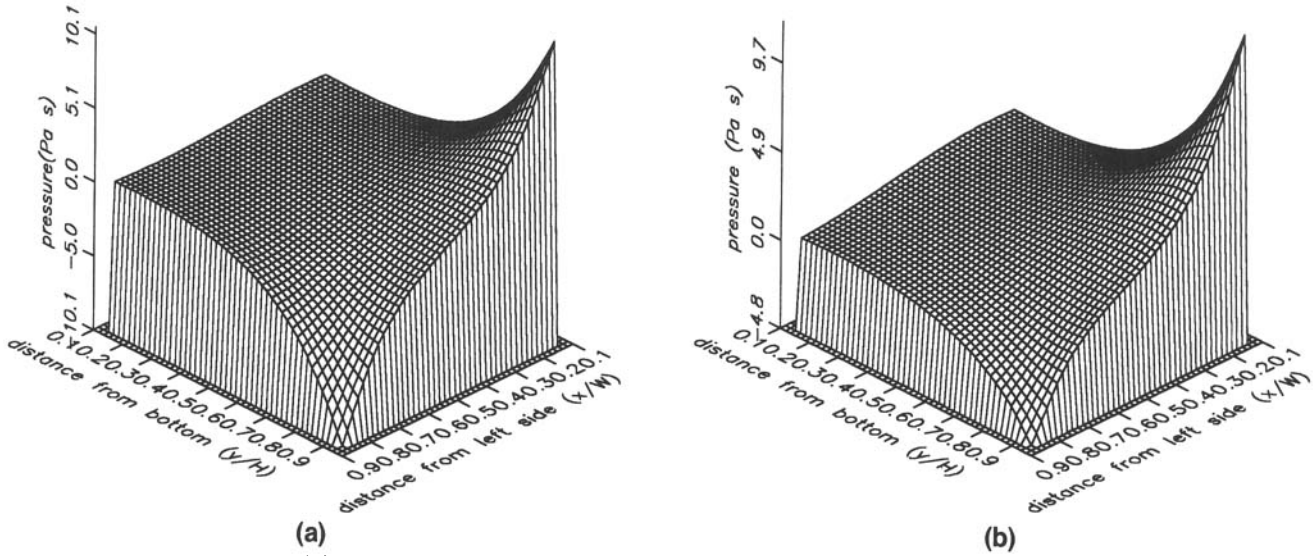

Figure 8. Pressure distributions across the channel.

(a) Fully-filled channel; (b) partially-filled channel.

Table 1. Normalized Cross-Channel Pressure Differences from This Model and Eq. 15

Aspect Ratio	Pressure Difference	
	By This Model	By Eq. 15
10	1.275	1
5	1.678	1
2	2.872	1
1	4.830	1

RTD in fully-filled screw channels

Computed examples of RTD functions in fully-filled channels of different aspect ratios are shown in Figure 9 along with the values of the minimum and the mean residence times. This comparison shows the magnitude of the errors to be expected when the traditional assumption of 1-D cross-channel flow is used for channels of finite aspect ratios. As can be concluded, the conventional analysis may be useful at best for channels with large W/H ratios; even in those cases, however, it fails to explain the transfer of the fluid from the barrel to the screw surface and vice versa. The "long tail" of the RTD function for channels with small aspect ratios is clearly noticeable, and it is not limited to the fully-filled channels. In either case, it may have significant effects on mass-transfer operations such as devolatilization and reactive extrusion.

The effects of the down-channel pressure gradient on RTD in the fully-filled channels are shown in Figure 10a for a channel of aspect ratio of 2.0, and in Figure 10b for an infinitely wide channel for reference.

Effect of free surface

The free surface in a partially-filled channel tends to reduce the flow stress and hence affects the RTD. Its significance depends again on the ratio of the channel-filled width and depth. When this ratio is reasonably large, say, of the order of unity, the free surface does not affect the RTD function appreciably (Figure 11a). Under these conditions, the

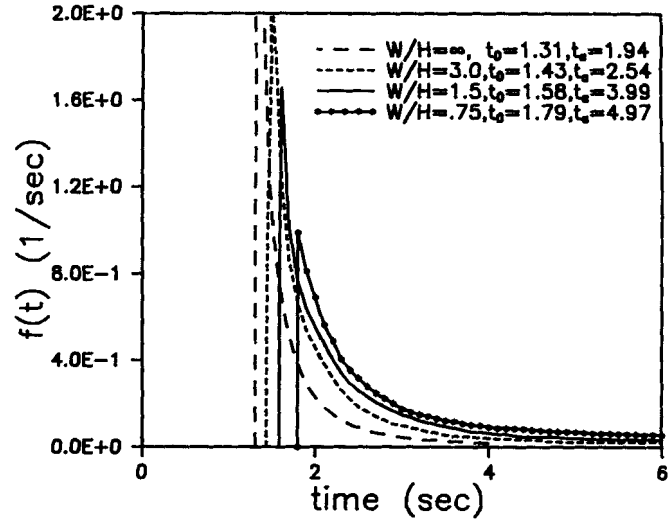

Figure 9. RTD functions obtained from Eqs. 12 and 14 for channels with different aspect ratio.

Screw speed $n = 60$ rpm; channel length depth ratio $L/H = 20$, helix angle $\theta = 17.6°$.

difference in the RTDs between the fully-filled and the partially-filled channel is small. However, the free surface does affect the RTD significantly when the W_s/H is small (Figure 11b). As indicated above, a secondary vortex tends to form in a fully-filled channel of an aspect ratio of 0.5 or less. On the other hand, the streamlines remain virtually unchanged in a partially-filled channel of the same aspect ratio, because the free surface does not hamper the flow as the stationary wall does. The long tail of the RTD function for the fully-filled channel shows why a poorly filled screw channel is usually not acceptable in extruder operations, particularly if chemical reaction is involved.

It is noted again that the free surface has been assumed to be a perfect plane, and that the complex effects of viscoelas-

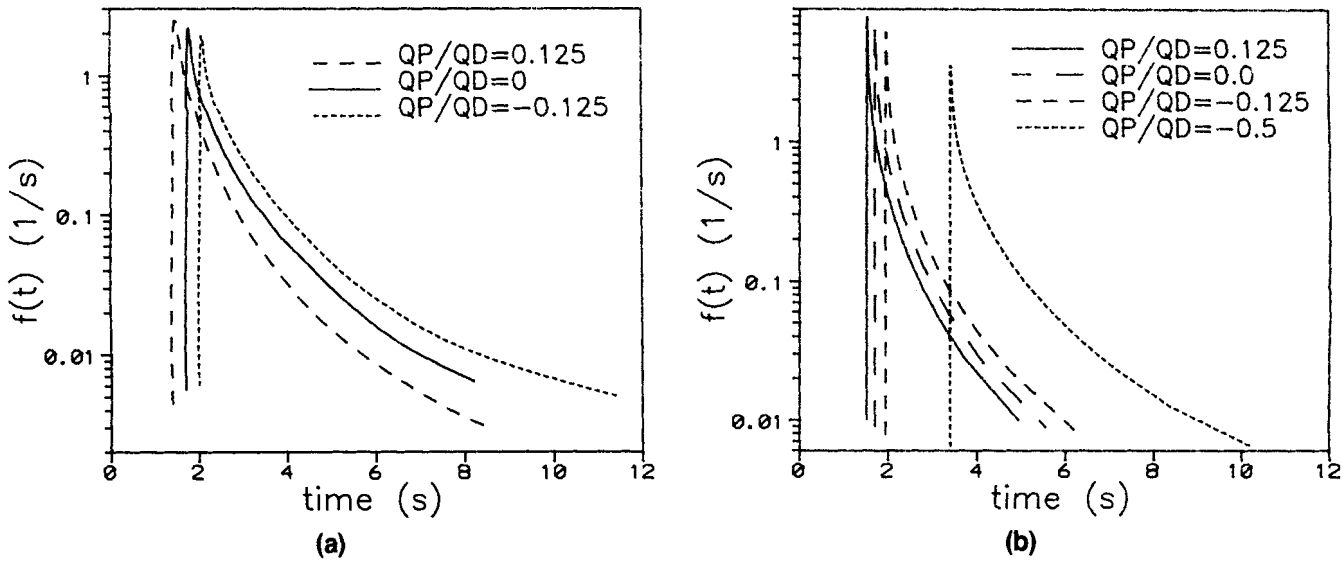

Figure 10. RTD functions at different down-channel pressure gradients.

Aspect ratio $W/H = 2.0$, the rest of operating conditions the same as in Figure 9.

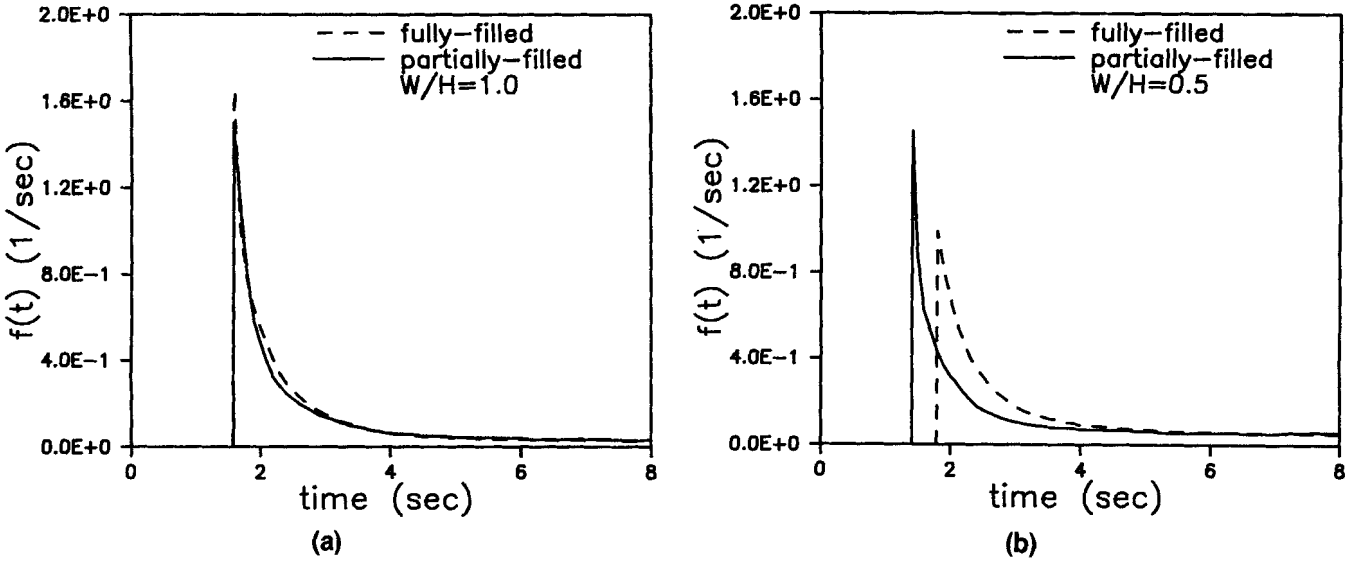

Figure 11. Comparison of RTD functions for fully- and partially-filled channels, with and without a free surface.

(a) $W/H = 1.0$; (b) $W/H = 0.5$.

ticity and surface tension have been neglected. The error introduced by these assumptions tends to be small if the filled width of the channel is relatively large ($W/H > 1$), but it is expected to grow when the degree of fill becomes small. An accurate determination of the actual position of the free surface remains a significant problem yet to be solved.

Conclusions

In this article, a Newtonian analysis of the cross-channel flow is given for both fully-filled and partially-filled screw channels. Using this description along with the conventional down-channel flow analysis, the residence time distribution (RTD) has been determined by tracing the streamlines within the resultant flow field. The following conclusions have been reached:

(1) The aspect (width/depth) ratio profoundly affects the RTD. The traditional assumption of fully-developed, 1-D cross-channel flow is useful mainly as a reference and for channels of large aspect ratios.

(2) For channel of small aspect ratios ($W/H < 1$), the following occurs. Secondary vortices tend to form at the bottom of the channel in fully-filled channels. The areas of stagnation flow tend to increase significantly while the RTD functions broaden accordingly, showing a pronounced "tail" at long times. In partially-filled channels, the corresponding streamlines remain largely unaffected as the free surface does not provide sufficient resistance to the circulatory flow.

(3) Stagnation flow tends to develop at the lower corners of the channel, in which the fluid travels slowly in all three directions. The size of the stagnation area is about 1/4 of the channel depth for a Newtonian fluid, implying that screws with rounded corners should preferably be used to eliminate the area of stagnation. The radius of curvature should be approximately $H/4$.

Acknowledgment

We are grateful for the financial support of Elf Atochem (France), DSM Research (Netherlands), Exxon Chemical Company and The Goodyear Tire & Rubber Company. The permission to use POLYCAD, granted by Polydynamics Incorporation, is also gratefully acknowledged.

Notation

b = temperature sensitivity coefficient, $°C^{-1}$
$f(t)$ = residence time density function, 1/s
H = channel depth, m
p = pressure, Pa
t = time, s
t_0 = minimum residence time, s
t_a = mean residence time, s
T = temperature, °C
T_0 = reference temperature, °C
v = velocity, m/s
v_{bx} = barrel velocity in x direction, m/s
v_{bz} = barrel velocity in z direction, m/s
v_x = velocity in x direction, m/s
v_y = velocity in y direction, m/s
v_z = velocity in z direction (down-channel), m/s
W = screw channel width, m
W_s = filled width in partially-filled channel, m
x = coordinate in channel width direction, m
y = coordinate in channel depth direction, m
z = coordinate in down-channel direction, m

Greek letters

γ = rate of strain, s^{-1}
Δx = step length in x direction, m
Δy = step length in y direction, m
η = non-Newtonian viscosity, $N \cdot s/m^2$
η_0 = power-law consistency index at reference temperature T_0, $N \cdot s^n/m^2$
θ = helix angle, rad
μ = Newtonian viscosity, Pa·s
ψ = stream function, s^{-1}

Literature Cited

Burggraf, O. R., "Analytical and Numerical Studies of the Structure of Steady Separated Flows," *J. Fluid Mech.*, **24**, 113 (1966).
Bernhardt, E. C., et al., *Processing of Thermoplastic Materials*, Reinhold, New York (1959).

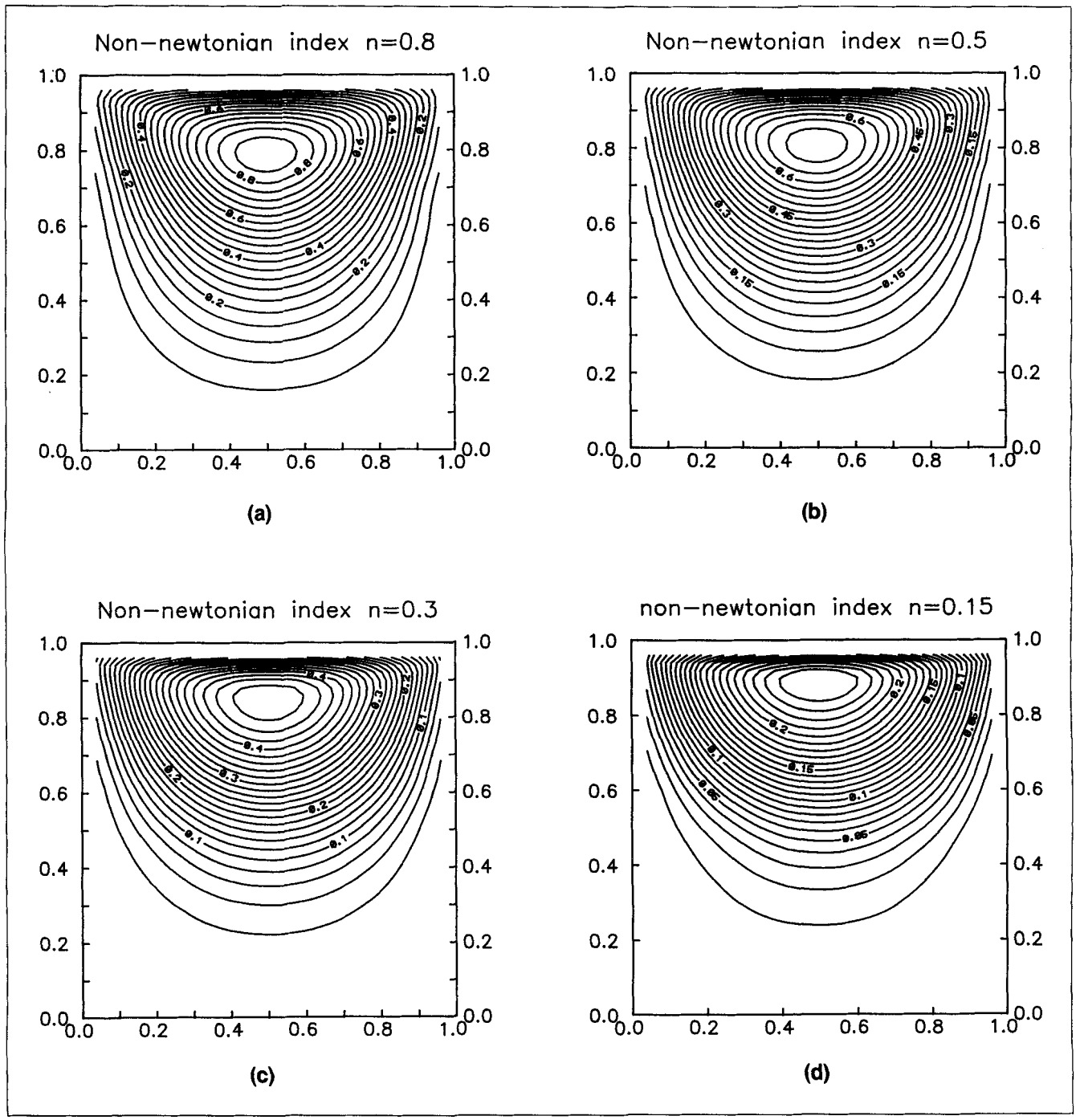

Figure A1. Streamlines in channels of aspect ratio $W/H = 1$ for a power law fluid.

(a) Non-Newtonian index $n = 0.8$; (b) $n = 0.5$; (c) $n = 0.3$; (d) $n = 0.15$.

Chen, L., et al., "Residence Time Distribution in Screw Extruders," *AIChE J.*, **39**(9), 1455 (Sept. 1993).

Kao, S. V., and G. R. Allison, "Residence Time Distribution in a Twin Screw Extruder," *Poly. Eng. Sci.*, **24**, 645 (1984).

Leong, C. W., and J. M. Ottino, "Experiments on Mixing Due to Chaotic Advection in a Cavity," *J. Fluid Mech.*, **209**, 463 (1989).

McKelvey, J. M., *Polymer Processing*, Wiley, New York, p. 235 (1962).

Tadmor, Z., and I. Klein, *Engineering Principles of Plasticating Extrusion*, Van Nostrand Reinhold, New York, p. 217 (1970).

Vlachopoulos, J., et al., "POLYCAD: A Finite Element Package for Molten Polymer Flow," *Applications of CAE in Extrusion and Other Continuous Processes*, K. T. O'Brien, ed., Carl Hanser Verlag (1991).

Appendix: Non-Newtonian Analysis of Cross-Channel Flow

The cross-channel flow of a non-Newtonian, nonelastic shear-thinning, fluid has been analyzed using the commercial software POLYCAD (Vlachopoulos, 1991). The power-law model was used in the following form

$$\eta = \eta_0 \left[\frac{1}{2} \sqrt{\dot{\gamma} : \dot{\gamma}} \right]^{n-1} \dot{\gamma} \exp[-b(T - T_0)] \qquad (17)$$

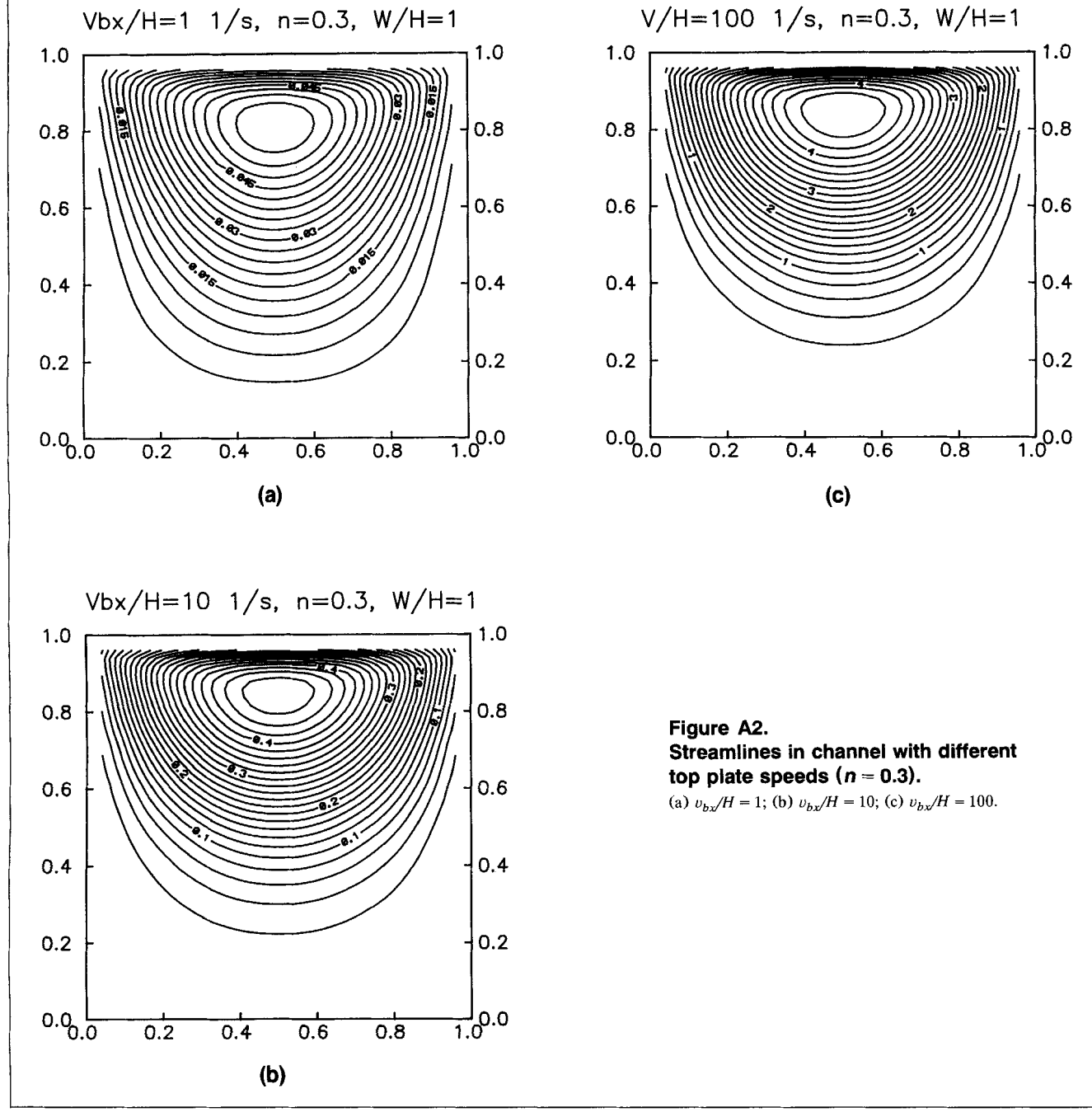

Figure A2.
Streamlines in channel with different top plate speeds ($n = 0.3$).
(a) $v_{bx}/H = 1$; (b) $v_{bx}/H = 10$; (c) $v_{bx}/H = 100$.

where η_0 is numerically equal to viscosity at the reference temperature of T_0 and a unit strain rate, $\dot{\gamma}$ is the rate of strain tensor, n is non-Newtonian index, and b is the temperature sensitivity coefficient.

The streamlines computed for the transverse flow in a square channel (aspect ratio $W/H = 1$) at the different non-Newtonian indices are shown in Figure A1. The influence of the top plate velocity V_{bx} (the barrel velocity) on the streamlines are shown in Figure A2. As expected, the streamlines for the power-law fluid are very close to those for a Newtonian fluid, if the non-Newtonian index is close to 1 and/or if the rate of deformation is small (Figure A1a and Figure A2a). The difference in streamlines becomes significant when the non-Newtonian index is small and the velocity V_{bx} is large (Figures A1b to A1d and Figures A2b and A2c). The size of the stagnation area at the bottom corners increases with a decrease in the non-Newtonian index and with an increase in the deformation rate, both producing a relative increase in viscosity in the area of low shear at the bottom of the channel. The effective viscosity differences between the bottom and top of the channel tend to restrict the cross-channel circulation. Indeed, this conclusion applies channels of all aspect ratios as illustrated in Figure A3 for a channel of $W/H = 10$.

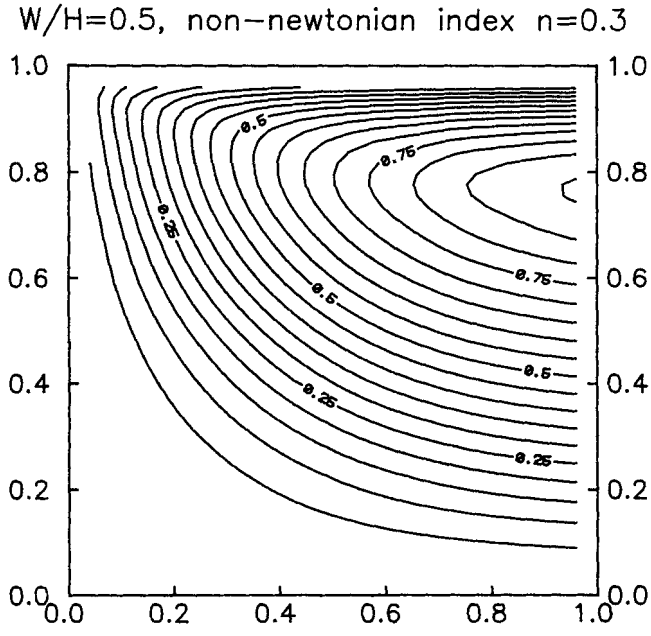

Figure A3. Streamlines in a wide channel ($W/H = 10$) for power law fluid ($n = 0.3$).

Table A1. Normalized Cross-Channel Pressure Differences for a Non-Newtonian Liquid

Non-Newtonian Index	Pressure Difference
1	4.945
0.8	4.362
0.5	3.383
0.3	2.480
0.15	1.588

Table A1 gives the results of the normalized cross-channel pressure difference for a fully-filled channel with a power law fluid predicted using POLYCAD. The definition of the normalized pressure difference is the same as Eq. 16 except the Newtonian viscosity η_0 is used. Note that the pressure difference decreases with the non-Newtonian index n, implying a smaller cross-channel pressure gradient and hence a slower recirculation. This further explains the increase of the stagnation area observed in Figures A2 and A3.

Manuscript received Jan. 10, 1995, and revision received Sept. 18, 1995.